Specification of Subunit Assembly by the Hydrophilic Amino-Terminal Domain of the Shaker Potassium Channel

Min Li, Yuh Nung Jan, Lily Yeh Jan

The functional heterogeneity of potassium channels in eukaryotic cells arises not only from the multiple potassium channel genes and splice variants but also from the combinatorial mixing of different potassium channel polypeptides to form heteromultimeric channels with distinct properties. One structural element that determines the compatibility of different potassium channel polypeptides in subunit assembly has now been localized to the hydrophilic amino-terminal domain. A *Drosophila* Shaker B (ShB) potassium channel truncated polypeptide that contains only the hydrophilic amino-terminal domain can form a homomultimer; the minimal requirement for the homophilic interaction has been localized to a fragment of 114 amino acids. Substitution of the amino-terminal domain of a distantly related mammalian potassium channel polypeptide (DRK1) with that of ShB permits the chimeric DRK1 polypeptide to coassemble with ShB.

Potassium channels display diverse kinetic properties, voltage dependence, and pharmacological properties (*1*) and are encoded by multiple genes (*2–5*). Some of the K^+ channel genes give rise to multiple protein products because of alternative splicing, thereby further increasing the diversity of K^+ channels (*6–8*). Other considerations for the generation of K^+ channel diversity include the assembly of K^+ channel subunits encoded by different genes or differentially spliced transcripts. Voltage-gated K^+ channel polypeptides contain a hydrophobic core region that includes several potential membrane spanning segments and is flanked by two hydrophilic cytoplasmic domains. Thus each K^+ channel polypeptide resembles one of the four internal repeats of the Na^+ or Ca^{2+} channel polypeptides and therefore would be likely to form tetramers (*2*, *9*). Certain combinations of K^+ channel polypeptides can coassemble and form heteromultimeric channels with distinct properties, offering a possible mechanism for further diversity (*10*, *11*). The Shaker, Shab, Shaw, and Shal K^+ channels in *Drosophila* and their homologs in other species form four subfamilies (*2–8*). Different members of the same subfamily share about 70 percent amino acid identity in the hydrophobic core region and can coassemble to form functional channels, whereas members of different subfamilies share about 40 percent amino acid identity but do not coassemble (*10–12*). It is not known how the compatibility between different K^+ channel polypeptides is determined. Similarly, most K^+ channel polypeptides appear capable of forming homomultimeric channels in *Xenopus* oocytes, but the structural elements involved in the interactions between identical K^+ channel subunits have not been identified. We report here the identification and characterization of a structural element that mediates K^+ channel subunit interactions and also determines the compatibility between different K^+ channel polypeptides in their ability to coassemble and form heteromultimeric channels.

The authors are in the Howard Hughes Medical Institute and Departments of Physiology and Biochemistry, University of California, San Francisco, CA 94143–0724.

Homophilic binding of the ShB K^+ channel amino-terminal domain. Members of the Shaker subfamily contain a highly conserved region within the hydrophilic NH_2-terminal domain (*2*, *3*, *5–7*). Although a deletion of this region in ShB, a K^+ channel polypeptide encoded by a *Shaker* splice variant (*6*), abolishes expression of K^+ current (*10*), the function of this conserved region has not been determined. To test whether this region has a role in subunit interaction, we looked for binding of ^{32}P-labeled soluble NH_2-terminal domain of ShB (NShB) to the full-length ShB polypeptide immobilized on a filter (*13*). The filter assay we used is a modification of the ones that have been used for detecting activities of a protein (such as DNA binding, kinase activity, peptide binding) after its immobilization on a membrane filter (*14*). The ShB K^+ channel NH_2-terminal domain (amino acids 1 to 227) (*6*) was produced, using the bacterial expression vector pAR.2HMK, as a fusion protein with the "FLAG" peptide tag and two heart muscle kinase recognition sites at the NH_2-terminus, thus allowing the fusion protein in the bacterial lysate to be labeled with

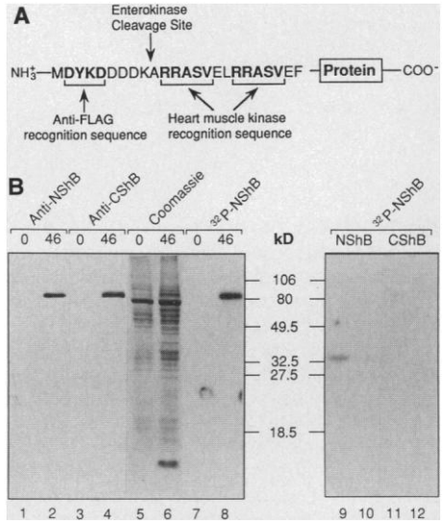

Fig. 1. Homophilic association of ShB NH_2-terminal hydrophilic domains (NShB) revealed by binding ^{32}P-labeled NShB fusion protein to immobilized ShB and NShB. (**A**) The fusion protein expressed in bacteria. At the NH_2-terminus of the fusion protein is a short peptide (the "FLAG"), which is recognized by the commercially available antibody to FLAG (anti-FLAG) (Immunex), and two heart muscle kinase sites. The expression vector used, pAR.2HMK, is derived from the pAR(ΔRI)59/60 vector (*14*), which includes a single heart muscle kinase site. The transcription was driven by T7 polymerase. Single letter amino acid codes are: A, Ala; R, Arg; N, Asn; D, Asp; C, Cys; Q, Gln; E, Glu; G, Gly; H, His; I, Ile; L, Leu; K, Lys; M, Met; F, Phe; P, Pro; S, Ser; T, Thr; W, Trp; Y, Tyr; V, Val. (**B**) Binding of NShB to ShB and NShB, but not to the COOH-terminal domain of ShB (CShB). Proteins (5 μg per lane) were fractionated by SDS-PAGE (lanes 1 to 12) and either visualized by Coomassie blue staining (lanes 5 and 6) or transferred to a nitrocellulose filter (lanes 1 to 4, 7 to 12): 0 and 46 represent total protein of SF9 cells at 0 and 46 hours after infection by the 3A1 strain of recombinant baculovirus carrying ShB cDNA (*15*). The labels NShB and CShB above the blot on the right indicate lysates of IPTG (isopropyl β-D-thiogalactoside)–induced (lanes 9 and 11) and noninduced (lanes 10 and 12) bacteria that contain the expression vector for IPTG-induced expression of NShB (residues 1 to 227) and CShB (residues 479 to 656) fusion protein, respectively. Rabbit antisera to NShB (anti-NShB) and CShB (anti-CShB) were obtained by immunizing the rabbits with purified NShB and CShB fusion protein, respectively. These antibodies (dilution, 1:10,000 and 1:500) were used in immunoblots (*28*). They specifically recognize the ShB polypeptide (82 kD) expressed in SF9 cells (lanes 1 to 4), as does ^{32}P-labeled NShB (lanes 7 and 8) (*13*). The NShB but not the CShB fusion protein is recognized by ^{32}P-labeled NShB (lanes 9 to 12).

[γ-^{32}P]ATP (adenosine 5′-triphosphate) by phosphorylation (Fig. 1A). Total lysate of SF9 cells infected with the 3A1 strain of recombinant baculovirus carrying ShB cDNA (*15*) was first fractionated by SDS–polyacrylamide gel electrophoresis (SDS-PAGE) and then transferred onto a nitrocellulose filter. After renaturation by a series of incubations with decreasing concentrations of guanidine-HCl, the immobilized protein was incubated with the ^{32}P-labeled soluble fusion protein. The ShB K^+ channel polypeptide was the only protein in the whole-cell lysate that was recognized by the ^{32}P-labeled ShB NH_2-terminal domain (Fig. 2B). This assay was specific and sensitive; picograms of ShB polypeptide could be detected, as indicated by titrations with purified ShB polypeptides (*16*).

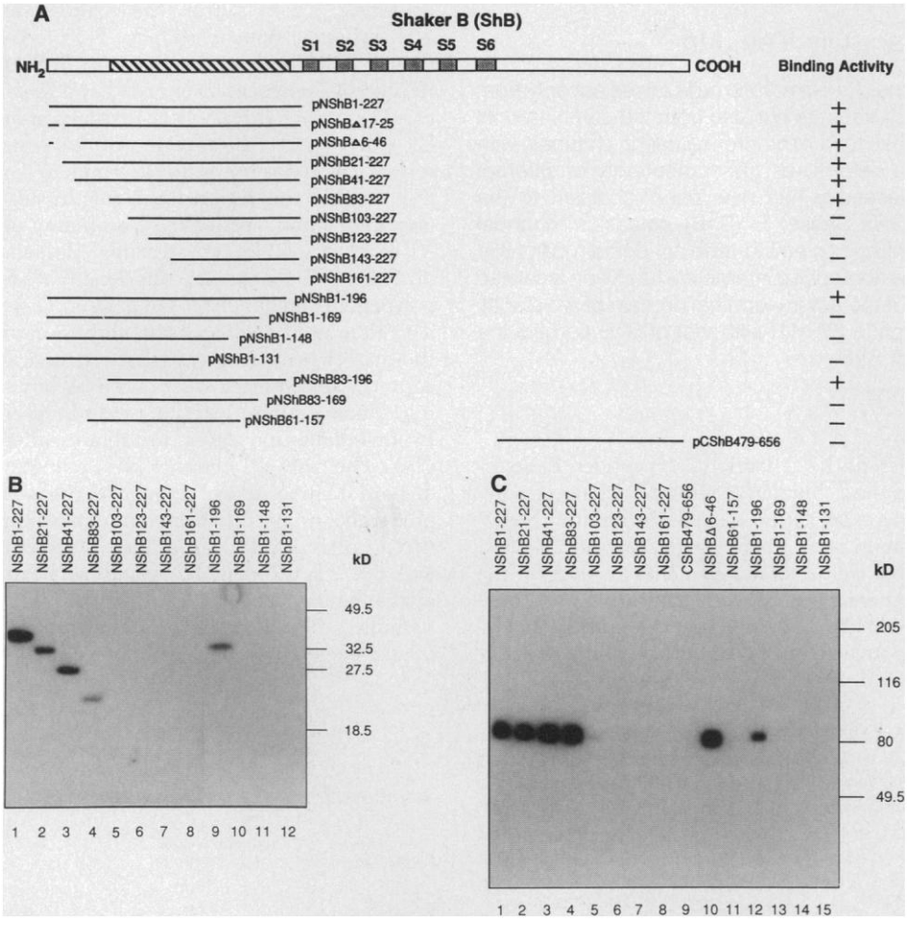

Fig. 2. A 114–amino acid fragment within the ShB NH_2-terminal domain (NShB) is required for the homophilic interaction. This was determined with ^{32}P-labeled NShB as a probe to test for binding to various fragments of NShB(B) or with these fragments as probes to test for their binding to ShB(C). (**A**) (Top) Diagram of the full-length ShB polypeptide. The shaded boxes represent the six putative transmembrane segments. The slashed box located in the hydrophilic NH_2-terminal domain represents amino acids 83 to 196. (Bottom) NShB, CShB, and fragments of NShB are produced with expression plasmids that include the coding sequences for the segments marked by the horizontal lines beneath the diagram of ShB. Numbers indicate the first and last amino acid residues in the fragment; pNShBΔ17-25 and pNShBΔ6-46 represent the NH_2-terminal domain (amino acids 1 to 227) with an internal deletion of amino acids 17 to 25 and amino acids 6 to 46, respectively. (+) Binding of the fragment to both ShB and NShB when used either as a probe or as an immobilized substrate; (−) no detectable binding in either case. The smallest fragment that shows binding contains amino acids 83 to 196. (**B**) Bacterial lysates containing equal amounts of various fragments of NShB (0.5 μg, as judged by the intensity of staining by Coomassie blue) were fractionated by SDS-PAGE; the fractions were immobilized on a nitrocellulose filter and tested for binding ^{32}P-labeled NShB (amino acids 1 to 227) (*13*). Deletion from the NH_2-terminus up to amino acid 83 did not abolish binding (lane 4). Deletion from the COOH-terminus up to amino acid 196 did not abolish binding (lane 9). (**C**) The total protein (25 μg) of the SF9 cell lysate obtained 46 hours after infection was placed in a single 8-cm-wide well, fractionated by 7 percent SDS-PAGE, and transferred to a nitrocellulose filter. Different fractions from this filter were exposed to different ^{32}P-labeled fragments of NShB or CShB, as indicated above each lane. These ^{32}P-labeled fragments were adjusted to the same specific activity and tested under identical conditions for their binding to ShB, the full-length K^+ channel polypeptide, again revealing that amino acids 83 to 196 correspond to the minimal requirement for the binding.

To identify the structural element of the ShB polypeptide that is recognized by the ShB NH_2-terminal domain, we expressed in bacteria the hydrophilic COOH-terminal domain (CShB), the NH_2-terminal domain, and a series of NH_2-terminal domain fragments that had different portions deleted (Fig. 2A). The corresponding coding sequences were obtained by polymerase chain reactions (PCR) in which appropriate pairs of oligonucleotide primers with flanking Eco RI restriction endonuclease sites were used. The PCR reactions were carried out with high copy number of template and low cycle number to reduce the chance of PCR amplification errors. The PCR products were cloned in frame into pAR.2HMK and then transformed into bacteria BL21(DE3)pLysS (F-ompTR_B-M_B-pLysS, Cm^r). For each construct, more than two independent clones were found to yield the same results when analyzed. The fusion proteins were expressed by inducing the bacterial culture with 1 mM IPTG for 4 hours at 37°C, and then labeled with ^{32}P or fractionated on SDS-PAGE for binding studies (*13*). The ^{32}P-labeled ShB NH_2-terminal domain bound to the NH_2-terminal but not the COOH-terminal domain (Fig. 1B). Moreover, the ^{32}P-labeled ShB COOH-terminal domain did not bind to the ShB polypeptide (Fig. 2C). Thus the interaction between the hydrophilic ShB NH_2-terminal domain and the full-length ShB polypeptide does not involve the hydrophilic COOH-terminal domain. It is possible that, in addition to the observed homophilic binding, the NH_2-terminal domain also interacts with sequences within the hydrophobic core region.

The minimal structural element required for the homophilic interaction of the ShB NH_2-terminal domain was determined by analyzing the binding of the ^{32}P-labeled ShB NH_2-terminal domain to various fragments of NH_2-terminal domain that were immobilized on a filter (Fig. 2B). To control for the possibility that some of these fragments might not be immobilized sufficiently to allow detection of their binding to the labeled domain, we also used each fragment as a ^{32}P-labeled probe to test for its ability to bind to the full-length ShB polypeptide immobilized on a filter (Fig. 2C). The minimal structural element identified in both cases corresponds to a 114–amino acid fragment (amino acids 83 to 196), which is shared by all known *Shaker* alternative splice variants (*2*, *6*, *7*). The sequence of this 114–amino acid fragment is also highly conserved (more than 70 percent amino acid identity) within the Shaker subfamily (*2*, *3*, *5*) (Fig. 3A). In-

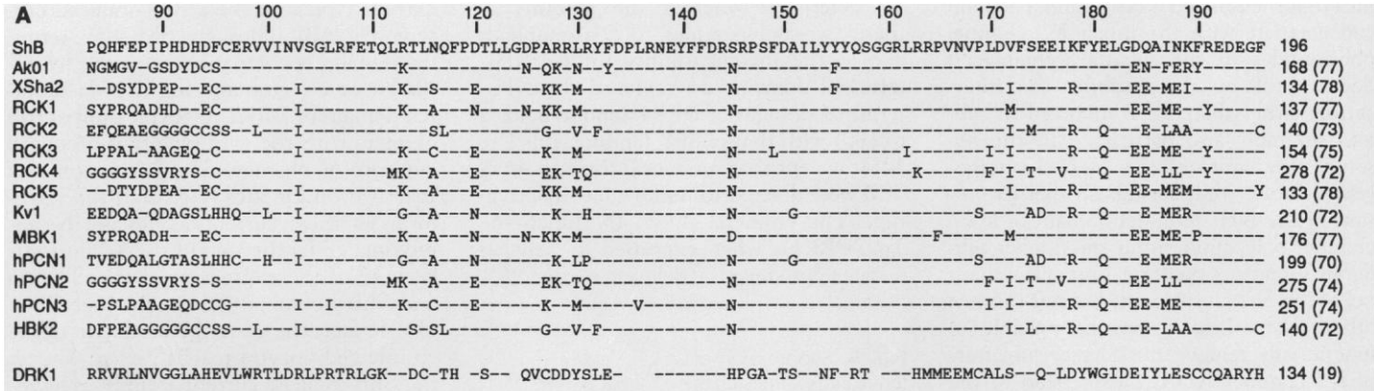

Fig. 3. The NH_2-terminal domains of different members of the Shaker subfamily are likely to be compatible for protein interactions. (**A**) Sequence conservation within the Shaker subfamily. The sequence required for NShB homophilic association is shown by single letter code. The amino acid sequences of known K^+ channel genes of the Shaker subfamily from different species (*Aplysia*, *Xenopus*, rat, mouse, and human) are aligned with the ShB sequence from *Drosophila* (*2–8*). A rat gene (DRK1, Shab subfamily) (*4*) is also included at the bottom. (–) The amino acid at that position is identical to that in the ShB sequence. Spaces in DRK1 sequence indicate gaps introduced. The name of each K^+ channel gene is given on the left of the sequence. The position of the last amino acid is identified by the number on the right. Numbers in parentheses indicate the percentage of identity to ShB sequence in the region shown. A similar alignment is given in (*30*). (**B**) Binding of the NH_2-terminal domains of ShB and RCK1, two members in the Shaker subfamily. The hydrophilic NH_2-terminal domain of RCK1(NRCK1, amino acids 1 to 167) was cloned and expressed as a fusion protein. Crude protein preparations (5 μg) of SF9 cell lysate (at 0 or 46 hours after infection) (lanes 1, 2, 5, and 6) and IPTG-induced bacterial lysate containing NH_2-terminal domains of ShB(NShB) or RCK1(NRCK1) (lanes 3, 4, 7, and 8) were fractionated by 11 percent SDS-PAGE. The fractionated protein samples were immobilized on nitrocellulose filters and incubated with ^{32}P-labeled NShB (lanes 1 to 4) or NRCK1 (lanes 5 to 8). As shown in these autoradiographs, ^{32}P-labeled NShB binds to NRCK1, ShB, and NShB. Likewise, ^{32}P-labeled NRCK1 shows homophilic binding as well as binding to ShB and NShB. The molecular size standards (in kilodaltons) are indicated between the two panels.

deed, the NH_2-terminal domain of a mammalian member of the Shaker subfamily, RCK1 (BK1 or Kv1.1) (*3*, *17*), also bound to ShB polypeptide and to the NH_2-terminal domain of either ShB or RCK1 (Fig. 3B). Furthermore, the pattern of binding of the RCK1 NH_2-terminal domain to various ShB NH_2-terminal domain fragments was identical to the one shown in Fig. 2B. This result is consistent with the finding that ShB and RCK1 can coassemble and form functional heteromultimeric channels (*10*).

Mutagenesis studies (*18*) have shown that the first 20 residues of the NH_2-terminus of ShB can act as the cytoplasmic inactivation gate (ball), which plugs the channel pore after channel opening and results in inactivation (*19*). Whereas deletion of residues 6 through 46 in ShB removes fast inactivation of the K^+ current, a peptide corresponding to the first 20 amino acids of ShB, when applied in solution from the cytoplasmic side of the membrane, restores fast inactivation (*18*). These sequences are present in only some of the *Shaker* alternative splice variants (*2*, *6*, *7*); they are not part of the 114–amino acid fragment required for the homophilic interaction of the NH_2-terminal domain. Further, an excess amount of the ShB NH_2-terminal peptide (amino acids 1 to 20) did not interfere with the homophilic binding of the ShB NH_2-terminal domain, indicating that the sequences that have been implicated as the fast inactivation gate are not involved in homophilic binding.

The only protein-protein interaction observed in our analysis was the homophilic binding of the NH_2-terminal domains. If this homophilic binding accounts for part of the subunit interactions of a K^+ channel, the ShB NH_2-terminal domain could be expected to form a homomultimer that contains the same number of subunits as does a K^+ channel. To test this possibility, we purified the ShB NH_2-terminal domain that was expressed in bacteria to homogeneity (Fig. 4) and examined its elution profile through a Superose 6 gel filtration column that yields size fractionation of molecules according to their Stoke's radius. Under high salt conditions, which were used to minimize possible nonspecific interactions between proteins, the purified NH_2-terminal domain was eluted from the column as two separate species (36 kD and 140 kD), corresponding to the size of a monomer and a multimer, respectively (Fig. 4). Sucrose gradient centrifugation of partially purified material containing the ShB NH_2-terminal domain also revealed the presence of a multimer as well as a monomer (*16*). The size of the multimer was consistent with that of a tetramer of the NH_2-terminal domain.

If indeed the isolated ShB NH_2-terminal domain can form multimers, co-expression of the NH_2-terminal domain with the ShB polypeptide may result in the binding of the hydrophilic NH_2-terminal domain to the full-length K^+ channel subunit in vivo. To test this notion, we constructed a truncated ShB cDNA that encodes the NH_2-terminal domain of ShB by deleting the coding sequence of ShB from amino acids 226 to 651, transcribed the RNA in vitro, and injected both RNA coding for the ShB NH_2-terminal domain and RNA coding for the full-length ShB into *Xenopus* oocytes. The expressed K^+ current was monitored by two-electrode voltage clamp recording, as described (*10*, *20*). Injection of twice the amount of RNA for the ShB polypeptide led to a doubling of the size of the K^+ current (Fig. 5, A and B), indicating that the amount of RNA injected did not saturate the biosynthetic machinery. However, injecting RNA for the entire ShB polypeptide together with an equivalent amount of RNA for the NH_2-terminal domain suppressed the functional expression of K^+ channels by a factor of 10 (Fig. 5C). Although these results are consistent with the

idea that the isolated NH_2-terminal domain can compete with the intact K^+ channel polypeptides in the subunit assembly, it does not rule out the possibility that interactions other than those involved in subunit assembly also participate in the observed dominant negative effect. Nonetheless, if future studies establish that expression of the NH_2-terminal domain of a K^+ channel polypeptide from the Shaker subfamily suppresses the formation of K^+ channel of the Shaker subfamily but not those of other subfamilies, it may be possible to functionally remove the Shaker subfamily of K^+ channels via the expression of the soluble NH_2-terminal domain.

Specification of heteromultimeric channel formation by the amino-terminal domain. Members of different K^+ channel subfamilies do not coassemble (*12*). Indeed, co-expression of ShB from the Shaker subfamily with the mammalian DRK1 (or Kv2.1) from the Shab subfamily (*4, 17*) gives rise to K^+ currents that are well fitted by the sum of the two currents that are produced by ShB (Fig. 6A) and DRK1 (Fig. 6C), respectively (Fig. 6, E and G).

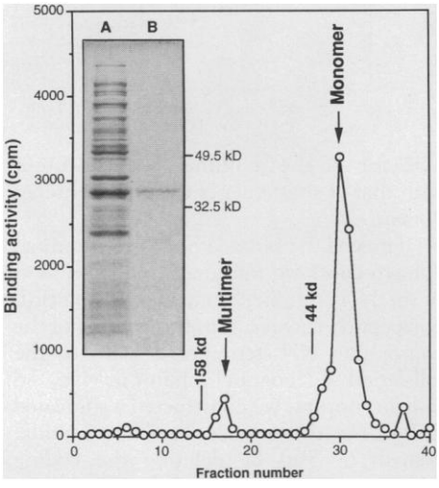

Fig. 4. Formation of a multimer by the ShB NH_2-terminal domain (NShB). After purification of the ShB NH_2-terminal domain from the bacterial lysate (*28*), the purified protein was analyzed by Superose 6 (FPLC) gel filtration column chromatography under high salt conditions (0.5 M KCl), and detection with ^{32}P-labeled NShB (*13*). The purified NShB eluted as two peaks with apparent molecular size as indicated, corresponding to the size of a monomer and a multimer, respectively. (Inset) SDS-PAGE of protein preparations visualized by Coomassie blue staining. (Lane A) Crude bacterial lysate (3 μg); (lane B) purified NShB (0.1 μg). Stoke's radius standards (Bio-Rad; thyroglobulin, 670 kD; γ-globulin, 158 kD; ovalbumin, 44 kD; myoglobulin, 17 kD; and vitamin B12, 1.35 kD) were fractionated under the same conditions and monitored by absorbance at 280 nm.

To determine whether the inability of these two polypeptides to coassemble is due to the incompatibility in the NH_2-terminal domain, we replaced the NH_2-terminal domain of DRK1 (amino acids 1 to 180) with that of ShB (amino acids 1 to 225), except that residues 6 through 46 of ShB were deleted to remove fast inactivation. This chimeric cDNA (NShBΔ6-46–TmCDRK1), when expressed in *Xenopus* oocytes, produced a delayed rectifier K^+ current typical of the DRK1-induced current (Fig. 6B). Thus, the ShB NH_2-terminal domain is compatible with the hydrophobic core region and the COOH-terminal domain of DRK1. Coexpression of this chimera with the wild-type ShB produced currents of characteristic activation and inactivation kinetics (Fig. 6D); the waveforms of these currents could not be approximated by the sum of the K^+ currents because of the expression of the chimera and ShB homomultimeric channels (Fig. 6F). In fact, the current recorded from the co-injected oocytes reached its peak after the ShB-induced current would have subsided, but before the rising phase of the chimera-induced current. At +60 mV the time to peak for the ShB current was 5.4 ± 0.4 ms (n = 7). The time to peak for the current recorded in oocytes that expressed both the ShB and the chimera was 21 ± 0.5 ms (n = 7). The time to peak for the chimera-induced current was greater than 100 ms (n = 5); this cannot be measured accurately because the current reached the plateau so slowly that there could be small contribution of slow activating currents intrinsic to the oocyte. Given this wide temporal separation between the peak current observed in co-injected oocytes and those in oocytes injected with either ShB or the chimera, the former is most likely due to coassembly of ShB and the chimera in the formation of

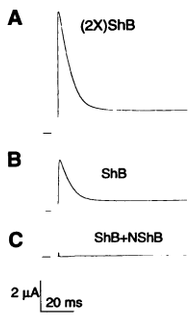

Fig. 5. Suppression of functional expression of the ShB K^+ current by the hydrophilic ShB NH_2-terminal domain. Within the linear range of ShB expression (A and B), injection of equal amount of ShB RNA and RNA for the hydrophilic NH_2-terminal domain of ShB (NShB) greatly suppressed the K^+ current (C). The currents were elicited by a 80-ms test pulse from −100 mV to +40 mV. The injected RNA's are (**A**) 50 ng of ShB RNA per oocyte, peak current 6.2 ± 1.5 μA, n (number of oocytes recorded) = 5; (**B**) 25 ng of ShB RNA per oocyte, peak current 2.9 ± 0.4 μA, n = 9; (**C**) 25 ng of ShB RNA and 25 ng of RNA coding for the first 225 and the last four residues of ShB per oocyte, peak current 0.2 ± 0.2 μA, n = 8.

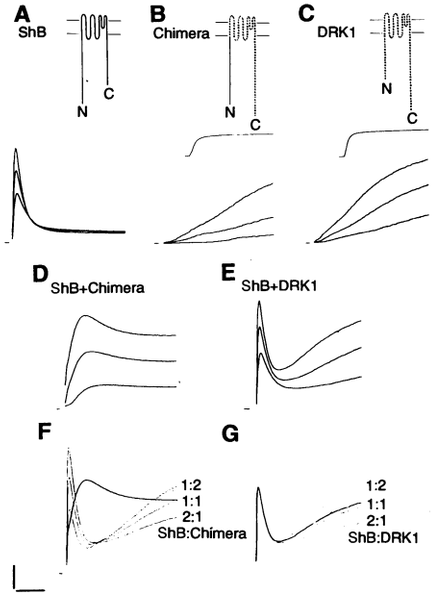

Fig. 6. Formation of functional heteromultimeric channels by ShB and a chimera of ShB and DRK1. This chimera, NShBΔ6-46–TmCDRK1, has the hydrophobic core region and the COOH-terminal domain of DRK1; the hydrophilic NH_2-terminal domain of DRK1 (amino acids 1 to 180) was replaced with that of ShB (amino acids 1 to 226), and an internal deletion of amino acids 6 to 46 of ShB was introduced to remove fast inactivation (**A** to **C**), when ShB is the solid line, and DRK1 is the dotted line. The chimera was functionally expressed in *Xenopus* oocytes and produced currents (B) that resembled the DRK1 K^+ current (C); in both cases the current activated much more slowly than the ShB K^+ current (A). Coexpression of ShB and the chimera gave rise to currents of waveform (**D**) different from those due to coexpression of ShB and DRK1 (**E**). (**G**) The current due to coexpression of ShB and DRK1 (elicited at +60 mV, solid line) is similar in waveform to that generated by digital addition of ShB and DRK1 currents (dotted lines, with ratios of the two currents indicated on the right of the traces); it matches the simulation of ShB:DRK1 = 1:1.2. (**F**) The current due to coexpression of ShB and the chimera (at +60 mV, solid line) does not match a simulation at any ratios. The currents were elicited by 85-ms test pulses at +20 mV, +40 mV, and +60 mV from a holding potential of −100 mV. The top traces in (B) and (C) were generated by 900-ms test pulses at +60 mV. The interval between test pulses was 3 seconds. The horizontal scale bar is 300 ms for inserted panels in (B) and (C) and 20 ms for all other traces. The vertical scale bar is 0.5 μA for (A), (D), and (E); 0.14 μA for (B); 0.24 μA for (C); 1.1 μA for the inserted panel in (B); and 1.9 μA for the inserted panel in (C). Each trace shown is representative of records from at least four oocytes.

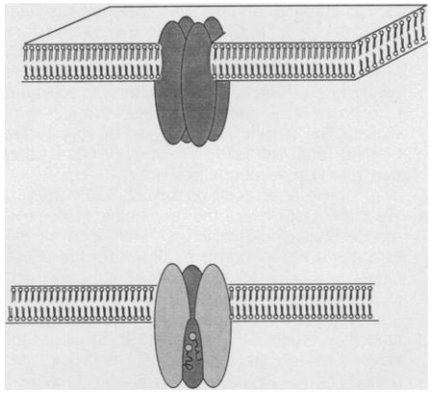

Fig. 7. A model for the Shaker K^+ channel. The channel appears to be a tetramer (*2*, *9*). The hydrophobic core region of each subunit contains the transmembrane segments and participates in pore formation. The hydrophilic NH_2- and COOH-terminal domains are on the cytoplasmic side. The interactions between subunits probably involve both the hydrophobic core region and the hydrophilic NH_2-terminal domain. The specificity of subunit association is determined by the NH_2-terminal domain. Also depicted is the cytoplasmic inactivation gate (ball and chain) (*18*, *19*). (Top) side view; (bottom) cross section.

heteromultimeric channels. These findings indicate that the hydrophobic core regions of DRK1 and ShB are compatible in the subunit interactions, even though they only share 40 percent amino acid identity; the failure of ShB and DRK1 to coassemble and form functional channels can be attributed to incompatible interaction between their hydrophilic NH_2-terminal domains.

The observed functional expression of NShBΔ6-46–TmCDRK1 and heteromultimer formation between this chimera and ShB may permit further extension of the structure-function analysis of K^+ channels. For example, it is now possible to analyze the voltage-gating of heteromultimeric channels composed of K^+ channel polypeptides which individually would give rise to homomultimeric channels with drastically different kinetic and voltage-dependent properties of activation. It may also be possible to replace the NH_2-terminal domain of DRK1 with that of the wild-type ShB polypeptide, and test whether the inactivation gate at the NH_2-terminus of this chimera would interact with a receptor that is conserved in DRK1 and is therefore also present in the chimera (*21*), thereby causing inactivation of this chimeric channel. If so, it would be possible to test for the coassembly of this NShB–TmCDRK1 chimera with the DRK1 polypeptide. If we assume that deletions of much of the hydrophilic sequences in both the NH_2- and COOH-terminal domains of DRK1 do not abolish functional expression (*22*), presumably because subunit interactions involving the hydrophobic core region of DRK1 are sufficient for homomultimeric channel formation, it should be feasible to determine whether these subunit interactions are counteracted by the incompatibility between the hydrophilic NH_2-terminal domains of the ShB and the DRK1 K^+ channel polypeptides.

K^+ channel subunit interactions. On the basis of our studies and those of others (*22*), we propose that the subunit interactions that support K^+ channel assembly involve the hydrophilic NH_2-terminal domain as well as the hydrophobic core region. The interactions involving the NH_2-terminal domain are homophilic so that a tetramer of the NH_2-terminal domains forms at the cytoplasmic side of the membrane and makes a vestibule at the cytoplasmic end of the channel pore (Fig. 7). The minimal structural element required for the homophilic interaction of the ShB NH_2-terminal domain is a 114–amino acid fragment. This structural element separates the cytoplasmic inactivation gate (*18*) from the structural elements associated with the voltage sensor (*23*), the pore-lining structures (*24*), and the receptor for the inactivation gate at the cytoplasmic mouth of the pore (*21*). No indications of any involvement of the hydrophilic COOH-terminal domains in the subunit interaction have been obtained.

How general might be the involvement of the NH_2-terminal domain in K^+ channel subunit interaction? Thus far, we find that the interactions involving the NH_2-terminal domain can account for the subunit interactions in homomultimers and heteromultimers that are composed of K^+ channel polypeptides of the Shaker subfamily. These interactions also allow heteromultimeric channel formation between ShB and the chimeric NShBΔ6-46–TmCDRK1, even though the wild-type ShB and DRK1, a mammalian K^+ channel polypeptide of the Shab subfamily, do not normally coassemble. It is not yet known whether homophilic binding of the NH_2-terminal domains of K^+ channel polypeptides of other subfamilies besides Shaker is involved in the formation of homomultimeric channels, or whether the incompatibility between members of the different K^+ channel subfamilies in the formation of functional heteromultimeric channels is generally due to incompatible interaction of their NH_2-terminal domains.

Some intriguing comparison can be made between K^+ channels and ligand-gated ion channels such as the nicotinic acetylcholine receptor. Whereas the acetylcholine receptor is a pentamer rather than a tetramer (*25*, *26*), it is likely that the extracellular NH_2-terminal domain participates in subunit interactions (*27*). Moreover, the acetylcholine receptor is a roughly cylindrical structure that extends from the membrane into the extracellular space, thereby forming a vestibule at the extracellular side of the channel pore (*25*). In this respect, we suggest that the K^+ channel may resemble an inverted acetylcholine receptor; the K^+ channel molecule might be expected to form a roughly cylindrical structure that extends from the membrane into the cytoplasm.

REFERENCES AND NOTES

1. R. Latorre, R. Corronado, C. Vergara, *Annu. Rev. Physiol.* **46**, 485 (1984); M. A. Rogawski, *Trends Neurosci.* **8**, 214 (1985); B. Rudy, *Neuroscience* **25**, 729 (1988); L. Y. Jan and Y. N. Jan, *Cell* **56**, 13 (1989); B. Hille, *Ionic Channels of Excitable Membranes* (Sinauer, Sunderland, MA, 1991).
2. B. L. Tempel, D. M. Papazian, T. L. Schwarz, Y. N. Jan, L. Y. Jan, *Science* **237**, 770 (1987).
3. B. L. Tempel, Y. N. Jan, L. Y. Jan, *Nature* **332**, 837 (1988); D. McKinnon, *J. Biol. Chem.* **264**, 8230 (1989); W. Stuhmer *et al.*, *EMBO J.* **8**, 3235 (1989).
4. G. C. Frech, A. M. J. Vandongen, G. Schuster, A. M. Brown, R. H. Joho, *Nature* **340**, 642 (1989).
5. S. Yokoyama *et al.*, *FEBS Lett.* **259**, 37 (1989); T. McCormack, E. C. Vega-Saenz de Miera, B. Rudy, *Proc. Natl. Acad. Sci. U.S.A.* **87**, 5227 (1990); A. Wei *et al.*, *Science* **248**, 599 (1990); J. Douglass *et al.*, *J. Immunol.* **144**, 4841 (1990); S. Grissmer, B. Dethlefs, J. J. Wasmuth, A. L. Goldin, G. A. Gutman, *Proc. Natl. Acad. Sci. U.S.A.* **87**, 9411 (1990); A. Grupe *et al.*, *EMBO J.* **9**, 1749 (1990); R. Swanson *et al.*, *Neuron* **4**, 929 (1990); K. G. Chandy *et al.*, *Science* **247**, 973 (1990); T. J. Baldwin, M.-L. Tsaur, G. A. Lopez, Y. N. Jan, L. Y. Jan, *Neuron* **7**, 471 (1991); M. D. Pak, M. Covarrubias, A. Ratcliffe, L. Salkoff, *J. Neurosci.* **11**, 869 (1991); M. D. Pak, K. Baker, M. Covarrubias, M. Butler, A. Ratcliffe, *Proc. Natl. Acad. Sci. U.S.A.* **88**, 4386 (1991); P. J. Pfaffinger, Y. Furukawa, B. Zhao, D. Dugan, E. R. Kandel, *J. Neurosci.* **11**, 918 (1991); L. H. Philipson *et al.*, *Proc. Natl. Acad. Sci. U.S.A.* **88**, 53 (1991); S. L. Roberds and M. M. Tamkun, *ibid.*, p. 1798; K. H. Schruter *et al.*, *FEBS Lett.* **278**, 211 (1991); P. M. Hwang, C. E. Glatt, D. S. Bredt, G. Yellen, S. H. Snyder, *Neuron* **8**, 473 (1992).
6. T. L. Schwarz, B. L. Tempel, D. M. Papazian, Y. N. Jan, L. Y. Jan, *Nature* **331**, 137 (1988).
7. A. Kamb, J. Tseng-Crank, M. A. Tanouye, *Neuron* **1**, 421 (1988); O. Pongs *et al.*, *EMBO J.* **7**, 1087 (1988).
8. C. J. Luneau *et al.*, *Proc. Natl. Acad. Sci. U.S.A.* **88**, 3932 (1991); C. J. Luneau, R. Wiedmann, J. S. Smith, J. B. Williams, *FEBS Lett.* **288**, 163 (1991).
9. R. MacKinnon, *Nature* **350**, 232 (1991).
10. E. Y. Isacoff, Y. N. Jan, L. Y. Jan, *ibid.* **345**, 530 (1990).
11. M. J. Christie, R. A. North, P. B. Osborne, J. Douglass, J. P. Adelman, *Neuron* **4**, 405 (1990); K. McCormack, J. W. Lin, L. E. Iverson, B. Rudy, *Biochem. Biophys. Res. Commun.* **171**, 1361 (1990); J. P. Ruppersberg *et al.*, *Nature* **345**, 535 (1990).
12. M. Covarrubias, A. Wei, L. Salkoff, *Neuron* **7**, 763 (1991); L. Salkoff *et al.*, *Trends Neurosci.* **15**, 161 (1992).
13. For protein binding analysis, the proteins were fractionated by SDS-PAGE and transferred to a nitrocellulose filter in a Laemmli buffer containing 20 percent methanol. The following steps were performed at 4°C: The filter was rinsed in buffer A (10 mM Hepes-KOH, pH 7.5, 60 mM KCl, 1 mM EDTA, 1 mM 2-mercaptoethanol) for 5 minutes. It was then exposed for 10 minutes each to buffer A supplemented with guanidine-HCl at decreasing concentrations: 6 M, 3 M, 1.5 M, 0.75 M, 0.38 M,

0.19 M, 0.1 M, and 0 M. The filter was then incubated for 60 minutes in buffer A supplemented with 5 percent dehydrated Carnation milk and 0.05 percent NP-40 and for another 60 minutes in the same buffer containing 1 percent rather than 5 percent dehydrated Carnation milk. The binding reaction was carried out by adding ^{32}P-labeled fusion protein to the buffer (10^6 cpm/ml) and incubating for 12 hours. For labeling fusion protein, the bacterial cells were collected by centrifugation and lysed by repeated freeze and thawing in buffer (20 mM Hepes-KOH, pH 7.5, 50 mM NaCl, 2 mM EDTA, and 0.2 percent deoxycholate). In most cases the fusion proteins represented at least 10 percent of the total bacterial protein. Protein preparations obtained after centrifugation at 12,000*g* for 20 minutes or further purification steps were incubated at 37°C for 90 minutes in a solution of 20 mM Hepes-KOH, pH 7.5, 100 mM NaCl, 12 mM $MgCl_2$, 1 mM dithiothreitol (DTT), 100 μCi of [γ-^{32}P]ATP, and 25 U of heart muscle kinase catalytic subunit (Sigma). The solution containing the phosphoproteins was then dialyzed against a buffer (10 mM Hepes-KOH, pH 7.5, 60 mM KCl, 1 mM EDTA, 1 mM DTT) to remove the unincorporated radioactivity. The specific activity of the ^{32}P-labeled protein was estimated to be 2.5 to 5.0 × 10^4 cpm/pmol of the polypeptide.

14. W. K. Miskimins *et al.*, *Proc. Natl. Acad. Sci. U.S.A.* **82**, 6741 (1985); D. R. Rawlins, G. Milman, S. D. Hayward, G. S. Hayward, *Cell* **42**, 859 (1985); J. E. Ferrell and G. S. Martin, *J. Biol. Chem.* **264**, 20723 (1989); B. R. Copeland, R. J. Richter, C. E. Furlong, *ibid.* **257**, 15065 (1982); M. A. Blanar and W. J. Rutter, *Science* **256**, 1014 (1992); W. S. Lee, C. C. Kao, G. O. Bryant, X. Liu, A. J. Berk, *Cell* **67**, 365 (1991).
15. K. Klaiber *et al.*, *Neuron* **5**, 221 (1990).
16. M. Li, Y. N. Jan, L. Y. Jan, unpublished data.
17. K. G. Chandy, *Nature* **352**, 26 (1991).
18. T. Hoshi, W. N. Zagotta, R. W. Aldrich, *Science* **250**, 533 (1990); W. N. Zagotta, T. Hoshi, R. W. Aldrich, *ibid.* **250**, 568 (1990); J. P. Ruppersberg *et al.*, *Nature* **352**, 711 (1991).
19. F. Bezanilla and C. M. Armstrong, *J. Gen. Physiol.* **70**, 567 (1977).
20. The recording was done in 88 mM NaCl, 2.4 mM $NaHCO_3$, 1 mM KCl, 0.82 mM $MgSO_4$, 0.41 mM $CaCl_2$, 0.33 mM $Ca(NO_3)_2$, 10 mM Hepes, pH 7.5 (the MBSH solution), 18° ± 1°C. Digital substraction of leak currents was done by using scaled average currents evoked by ten 20-mV hyperpolarizing pulses from the holding potential of −100 mV.
21. E. Y. Isacoff, Y. N. Jan, L. Y. Jan, *Nature* **353**, 86 (1991).
22. A. M. J. VanDongen, G. C. Frech, J. A. Drewe, R. H. Joho, A. M. Brown, *Neuron* **5**, 433 (1990).
23. G. A. Lopez, Y. N. Jan, L. Y. Jan, *ibid.* **7**, 327 (1991); E. R. Liman, P. Hess, F. Weaver, G. Koren, *Nature* **353**, 752 (1991); D. M. Papazian, L. C. Timpe, Y. N. Jan, L. Y. Jan, *ibid.* **349**, 305 (1991).
24. R. MacKinnon and G. Yellen, *Science* **250**, 276 (1990); H. A. Hartmann *et al.*, *ibid.* **251**, 942 (1991); G. Yellen, M. E. Jurman, T. Abramson, R. MacKinnon, *ibid.*, p. 939; A. J. Yool and T. L. Schwarz, *Nature* **349**, 700 (1991); L. Heginbotham and R. MacKinnon, *Neuron* **8**, 483 (1992); M. P. Kavanaugh *et al.*, *ibid.*, p. 493; G. E. Kirsch *et al.*, *ibid.*, p. 499.
25. N. Unwin, *Neuron* **3**, 665 (1989).
26. E. Cooper, S. Couturier, M. Ballivet, *Nature* **350**, 235 (1991).
27. Y. Gu *et al.*, *Neuron* **6**, 879 (1991); X. M. Yu and Z. W. Hall, *Nature* **352**, 64 (1991); S. Verrall and Z. W. Hall, *Cell* **68**, 23 (1992).
28. For immunoblots protein was fractionated by SDS-PAGE and transferred onto a nitrocellulose filter. The filter was incubated in a blocking solution [10 mM tris, pH 8, 150 mM NaCl, 1 percent Tween 20, 2 percent bovine serum albumin (BSA), 3 percent normal goat serum] for 30 minutes at room temperature. Binding to primary antibodies was effected by adding the rabbit antiserum to the blocking solution and incubating for 30 minutes at room temperature. The excess unbound antibodies were removed with TST solution (blocking solution without BSA and normal goat serum). The binding to secondary antibodies [horseradish peroxidase (HRP)–conjugated goat antibodies to rabbit immunoglobulin G (Amersham)] was performed in TST solution with a dilution of 1:10,000. The specific antibody binding was visualized by chemiluminescence (ECL system, Amersham).
29. The bacteria cell pellet was resuspended in buffer of 50 mM Hepes-KOH, pH 7.5, 100 mM KCl, 2 mM EDTA, 1 mM DTT, and 0.5 percent deoxycholate. The cell lysate was prepared by sonicating the cell suspension at medium scale twice for 30 seconds. Nucleic acid in the lysate was precipitated by polyamine and cleared by 20 minutes of centrifugation at 10,000*g*. This starting material was then fractionated on a Fast Protein Liquid Chromatography (FPLC) Mono Q (Pharmacia LKB) column with a 50 mM to 500 mM linear gradient of KCl. The activity was monitored by immunoblot (*28*) and the activity pool was then fractionated on FPLC phenol Sepharose with a 2 M to 100 mM linear gradient of $(NH_4)_2SO_4$ or directly purified through affinity column containing antibodies to the FLAG peptide tag (IBI), which recognize the peptide sequence DYKD (Fig. 1A). The activity was then concentrated by hydroxylapitite chromatography. This material was then analyzed on a FPLC Superose 6 column with a buffer containing 25 mM Hepes-KOH, pH 7.5, 0.5 M KCl, 2 mM EDTA, 2 mM DTT, and 5 percent (w/v) glycerol. The fraction collector was activated to collect 500 μl per fraction after the first 5-ml elution. The activity was followed by membrane binding analysis with ^{32}P-labeled NShB and quantified by spectrometry.
30. J. A. Drewe *et al.*, *J. Neurosci.* **12**, 538 (1992).
31. We thank C. Miller for the recombinant baculovirus for Shaker expression, D. McKinnon for the BK1 clone, R. Joho and A. Brown for the DRK1 clone, R. Aldrich for the pShB(Δ6-46) construct, M. Blanar for the pAR(ΔRI)59/60 vector, L. Qin for advice on tissue culture and immunoassays, E. Isacoff, Y. Kubo, G. Lopez, and P. Slesinger for advice on electrophysiological recording, M. Doherty for oligonucleotide synthesis, L. Ackerman for photography, B. Bannerman for typing the manuscript, and G. Feger, E. Giniger, E. Isacoff, A. Jarman, Y. Kubo, M. Sheng, V. Siegel, P. Slesinger, and M-L. Tsaur for comments on the manuscript. Supported by a Helen Hay Whitney Foundation fellowship (M.L.), the Muscular Dystrophy Association (M.L.), and the Howard Hughes Medical Institute (Y.N.J. and L.Y.J.).

11 May 1992; accepted 9 July 1992

Controlling Cardiac Chaos

Alan Garfinkel, Mark L. Spano, William L. Ditto, James N. Weiss

The extreme sensitivity to initial conditions that chaotic systems display makes them unstable and unpredictable. Yet that same sensitivity also makes them highly susceptible to control, provided that the developing chaos can be analyzed in real time and that analysis is then used to make small control interventions. This strategy has been used here to stabilize cardiac arrhythmias induced by the drug ouabain in rabbit ventricle. By administering electrical stimuli to the heart at irregular times determined by chaos theory, the arrhythmia was converted to periodic beating.

The realization that many apparently random phenomena are actually examples of deterministic chaos offers a better way to understand complex systems. Phenomena that have been shown to be chaotic include the transition to turbulence in fluids (*1*), many mechanical vibrations (*2*), irregular oscillations in chemical reactions (*3*), the rise and fall of epidemics (*4*), and the irregular dripping of a faucet (*5*). Several studies have argued that certain cardiac arrhythmias are instances of chaos (*6*, *7*). This is important because the identification of a phenomenon as chaotic may make new therapeutic strategies possible.

Until recently the main strategy for dealing with a system displaying chaos was to develop a model of the system sufficiently detailed to identify the key parameters and then to change those parameters enough to take the system out of the chaotic regime. However this strategy is limited to systems for which a theoretical model is known and that do not display irreversible parametric changes (often the very changes causing the chaos) such as aging.

Recently a strategy has emerged that does not attempt to take the system out of the chaotic regime but uses the chaos to control the system. The key to this approach lies in the fact that chaotic motion includes an infinite number of unstable periodic motions (*8*). A chaotic system never remains long in any of these unstable motions but continually switches from one periodic motion to another, thereby giving the appearance of randomness. Ott, Grebogi, and Yorke (OGY) (*9*) postulated that it should be possible to stabilize a system around one of these periodic motions by using the defining feature of chaos, the extreme sensitivity of chaotic systems to perturbations of their initial conditions.

The OGY theory was first applied experimentally to controlling the chaotic vibrations of a magnetoelastic ribbon (*10*) and subsequently to a diode resonator circuit

A. Garfinkel is in the Department of Physiological Science, University of California, Los Angeles, CA 90024–1527. M. L. Spano is at the Naval Surface Warfare Center, Silver Spring, MD 20903. W. L. Ditto is in the Department of Physics, The College of Wooster, Wooster, OH 44691. J. N. Weiss is in the Department of Medicine (Cardiology), University of California, Los Angeles, CA 90024.